# Biochemical and biophysical characterization of human recombinant lecithin:cholesterol acyltransferase

**Lihua Jin, Young-Phil Lee, and Ana Jonas**[1]

Department of Biochemistry, University of Illinois at Urbana-Champaign, 506 South Mathews Avenue, Urbana, IL 61801

**Abstract** We established a Chinese hamster ovary cell line that constitutively expresses up to 5 mg/L of human recombinant lecithin:cholesterol acyltransferase (rLCAT). We purified the rLCAT to > 96% purity, and characterized it along with plasma LCAT (pLCAT) biochemically and biophysically. The recombinant enzyme is more heavily glycosylated and more heterogeneous in its carbohydrate content than the plasma enzyme, as revealed by differences in molecular weight and pI isoforms, determined by mass spectrometry and isoelectric focusing. Recombinant LCAT is half as active enzymatically as pLCAT. The difference in activity is due to differences in the catalytic rates rather than in the apparent $K_m$ values, suggesting that the binding of the rLCAT to interfaces is not altered by its different glycosylation pattern. Despite these differences, rLCAT has essentially the same intrinsic tryptophan fluorescence emission spectrum and far-UV CD spectrum as pLCAT, indicating that the tertiary and secondary structures of both enzyme forms are very similar. Both enzyme forms have a propensity to self-associate, and their multimers appear resistant to dissociation by SDS and dilution. The free energies of unfolding ($\Delta G_{(H_2O)}$) of rLCAT and pLCAT are 3.4 ± 0.2 and 3.2 ± 0.2 kcal/mol, respectively, as determined by guanidine hydrochloride denaturation monitored by fluorescence. These relatively low $\Delta G_{(H_2O)}$ values support the notion that LCAT is capable of undergoing major conformational changes upon interaction with interfacial substrates.—**Jin, L., Y-P. Lee, and A. Jonas.** Biochemical and biophysical characterization of human recombinant lecithin:cholesterol acyltransferase. *J. Lipid Res.* 1997. **38:** 1085–1093.

**Supplementary key words** CHO cells • plasma lecithin:cholesterol acyltransferase • glycosylation • fluorescence • circular dichroism • free-energy of denaturation

Lecithin:cholesterol acyltransferase (LCAT) is a key enzyme in the metabolism of high density lipoproteins and in reverse cholesterol transport, the pathway by which peripheral cell cholesterol is returned to the liver for catabolism [for reviews, see Jonas (1, 2); Fielding and Fielding (3)]. LCAT catalyzes the transfer of an acyl group from the *sn*-2 position of phosphatidylcholine (PC) to the 3-hydroxyl group of cholesterol, forming cholesteryl ester and lyso-PC. This reaction occurs preferentially on the surface of high density lipoproteins (HDL), where LCAT is activated by the major protein component of HDL, apolipoprotein A-I (apoA-I).

LCAT is synthesized in the liver and secreted into the plasma. The mature protein of human plasma LCAT (pLCAT) is a single polypeptide chain of 416 amino acids with a calculated polypeptide molecular weight of 47,090 (4). LCAT is glycosylated at all four potential N-linked glycosylation sites (Asn-20, 84, 272, and 384) (5–9), leading to a carbohydrate content of approximately 25% of total mass as determined by carbohydrate analysis (10–12). More recently, O-glycosylation sites were also reported for LCAT at $Thr^{407}$ and $Ser^{409}$ (13). The apparent molecular weight of plasma LCAT, estimated with SDS-PAGE and sedimentation equilibrium methods, ranges from 59 to 68 kDa (10, 11, 14–16). LCAT is known to lose activity easily in high salt buffer at the air/water interfaces (17), but quantitative protein stability data is not yet available. CD studies of LCAT have indicated the presence of 18–24% α-helix, 30–53% β-sheet, and 29–46% random structure (14, 15).

Mutagenesis studies have identified $Ser^{181}$ as the catalytic Ser of LCAT (18), and have demonstrated that the two free cysteines ($Cys^{31}$ and $Cys^{184}$) may be located near the active site, but are not involved in the catalytic

Abbreviations: LCAT, lecithin:cholesterol acyltransferase; PC, phosphatidylcholine; HDL, high density lipoproteins; apoA-I, apolipoprotein A-I; pLCAT, plasma LCAT; rLCAT, recombinant LCAT; *dhfr*, dihydrofolate reductase; α-MEM, modified Eagle's medium; FBS, fetal bovine serum; MTX, methotrexate; rHDL, reconstituted HDL; $BS^3$, bis (sulfosuccinimidyl) suberate; sulfo-EGS, ethylene glycobis (sulfosuccinimidyl) succinate; $\lambda_{max}$, wavelength maximum; GdnHCl, guanidine hydrochloride; CE, cholesteryl ester.

[1]To whom correspondence should be addressed.

mechanism (19). Various natural mutations in human plasma LCAT have been linked to the genetic disorders of familial LCAT deficiency and fish-eye disease (20–23); and several of these mutations have been expressed in animal cells to confirm the functional effects of the LCAT defects (24, 25). Our laboratory recently constructed C-terminal deletion mutants of LCAT to study their effects on LCAT secretion from COS-1 cells and on LCAT enzymatic activities (26). And Subbaiah and colleagues (27) produced a chimeric human/mouse LCAT with altered substrate specificity for phosphatidylcholine acyl chains. However, further studies on structure–function relationships of LCAT or on the physical properties of LCAT have been limited by the difficulty in producing sufficient amounts of plasma or recombinant LCAT. Hill et al. (28) first reported the stable expression and purification of human recombinant LCAT (rLCAT), on the order of 10 mg/L, in a baby hamster kidney (BHK) cell line, and described a simple enzyme purification procedure. We have established a Chinese hamster ovary (CHO) cell line that constitutively expresses up to 5 mg/L of human recombinant LCAT. We now report the purification of rLCAT from this cell line using a procedure adapted from Hill et al. (28) and describe data on the biophysical and biochemical properties of the recombinant and the plasma LCAT.

This work forms the background of ongoing mutagenesis studies in our laboratory into the structural basis of LCAT binding to interfaces, its activation by apoA-I, and its catalytic mechanism.

## MATERIALS AND METHODS

### Cell culture

The LCAT expression vector pSVDNALCAT (Kozak) containing human LCAT and *dhfr* cDNAs was previously constructed in this laboratory (26). The LCAT expression vector was transfected into CHO/*dhfr*$^-$ cells by the calcium phosphate method. After the transfected cells reached confluency, the cells containing the vector were selected using nucleoside-deficient minimal Eagle's medium (α-MEM) containing 10%-dialyzed fetal bovine serum (FBS). Large colonies growing well in the selective medium were transferred to 60-mm plates. When the cells reached confluency, they were split into the selective media containing 0.02 μM methotrexate (MTX) for concomitant amplification of the LCAT gene and the *dhfr* gene. The culture medium was also collected from the confluent cells for LCAT activity assay, after changing to Opti-MEM I medium (Gibco-BRL) in order to reduce background from serum. To obtain stable cell lines in which the amplified LCAT genes are integrated into chromosomes takes several months of growth in progressively increasing concentrations of methotrexate from the initial 0.02 μM to concentrations of up to 10.2 μM. The following culture conditions for transfected cells were adapted from Hill et al. (28). LCAT-CHO cells (~$6 \times 10^6$) amplified in 10.2 μM MTX were mixed with 1 g porous microcarrier beads (Cultispher-G, HyClone Laboratories, Inc., Logan, UT) and incubated with 1-min manual mixing every 3–4 h at 37°C under 5% $CO_2$ in 500 ml α-MEM (Gibco-BRL) containing 10% dialyzed FBS, 10.24 μM MTX (Gibco-BRL), 100 units/ml penicillin, and 100 μg/ml streptomycin (referred to as α-MEM in the following text). After the initial 24-h incubation period, 500 ml fresh α-MEM was added and the culture suspension was incubated with stirring at 15 rpm for 5 days. The medium was then changed to Opti-MEM I reduced serum medium (Gibco-BRL) supplemented with 10.24 μM MTX, penicillin, and streptomycin (concentrations as above). The cell suspension was incubated for 72 h before the culture medium was collected for rLCAT purification.

### Purification of rLCAT

The procedure for the purification of rLCAT was adapted from the method described by Hill et al. (28) and was carried out at 4°C. The culture medium was filtered through a 0.22-μm filter and was passed through a 1.6 × 20 (cm) phenyl Sepharose CL-4B (Pharmacia) column pre-equilibrated with 5 mM sodium phosphate buffer (pH 7.4) and 0.3 M NaCl. The column was washed with the same buffer until absorbance at 280 nm was below 0.005. Subsequently, rLCAT was eluted with deionized water. The rLCAT fractions were pooled and dialyzed against 5 mM Na phosphate buffer, pH 7.4, 5 mM EDTA. Residual bovine serum albumin was removed by passing the enzyme preparation through an (1 × 15 cm) Affigel-blue column pre-equilibrated with 10 mM TrisHCl, 5 mM EDTA, 50 mM NaCl, pH 7.6. While albumin bound tightly to the column, rLCAT passed through. The eluted rLCAT was pooled, concentrated with Centricon/10 (Amicon), and stored in the same buffer.

LCAT activity measurements were performed using reconstituted high density lipoprotein (rHDL) particles, which were prepared with egg phosphatidylcholine/[$^{14}$C]cholesterol/apoA-I in 100:5:1 molar ratios by the cholate dialysis method (29, 30). The activity assays were described previously (31). Samples contained from 2.0 to 20.0 μg of apoA-I in rHDL, BSA and β-mercaptoethanol in a total volume of 0.45 ml in 10 mM Tris-HCl buffer (pH 8.0), 150 mM NaCl, 1 mM $NaN_3$, 0.01%

EDTA. An appropriately diluted sample (to give linear product formation) of purified rLCAT, pLCAT, or culture medium (50 μl) was added to the substrate and incubated for 30 min at 37°C. The reactions were stopped with 5 ml of chloroform–methanol 2:1 (v/v) containing unesterified cholesterol and cholesteryl ester of 40 μg/ml each. The unesterified cholesterol and the cholesteryl ester were separated using instant thin-layer chromatography (ITLC) (Gelman Sciences), and the radioactivity was quantitated by scintillation counting. The kinetic data were analyzed using both a fit to a hyperbolic Michaelis-Menten curve and to a linear Lineweaver-Burk plot to obtain the apparent kinetic constants.

### Electrophoresis and immunoblotting

Native, SDS, and isoelectric focusing gel electrophoresis was performed using PhastGels (Pharmacia) on Pharmacia's PhastSystem at 15°C unless specified otherwise. For denaturing gels, the samples were denatured by boiling for 5 min in the presence of 3% SDS and cooled down on ice unless specified otherwise. For protein purity assessment, samples were overloaded in order to detect small amounts of contaminating proteins. Proteins were visualized by silver staining and, whenever necessary, gels were scanned using the Ultroscan XL Laser Densitometer (LKB Bromma) for protein quantitation.

For immunoblotting, protein samples were separated on a 7.5% SDS PhastGel (Pharmacia) and subsequently transferred to nitrocellulose membranes using Pharmacia's semi-dry transfer cell coupled to the PhastSystem gel-running apparatus. The membrane was treated with goat anti-LCAT antibodies followed by horseradish peroxidase-conjugated IgG. LCAT bands were visualized with the substrate 3,3′-diaminobenzidine tetrahydrochloride.

### N-terminal sequencing

The rLCAT was run on a 10% SDS polyacrylamide gel. Protein bands were electroblotted onto a polyvinyllidene difluoride (PVDF) membrane, and were stained with Coomassie blue R-250.

N-terminal sequence analysis of rLCAT was carried out in the Biotechnology Center, University of Illinois at Urbana-Champaign, by performing Edman degradation on an Applied Biosystems Model 477A instrument.

### Chemical cross-linking

The chemical cross-linking experiments were carried out for rLCAT in the presence of 70 mM freshly prepared bis(sulfosuccinimidyl) suberate ($BS^3$) (Pierce) or 70 mM ethylene glycobis(sulfosuccinimidyl) succinate (sulfo-EGS) (Pierce) in 12.5 mM sodium phosphate buffer (pH 7.4), 0.45% NaCl, 0.005% EDTA, and 0.01% $NaN_3$. Protein concentration in the reaction ranged from 0.010 to 0.75 mg/ml. Reaction mixtures were incubated at room temperature for 4.5 h, and were then concentrated using SpeedVac to a final protein concentration of 1.0 mg/ml. Reaction products were analyzed on 7.5% SDS gels (PhastSystem, Pharmacia) where each lane was loaded with equal amounts of protein. Proteins were silver-stained, and the gels were scanned.

### Deglycosylation reaction and mass spectrometry

Both pLCAT and rLCAT were denatured by boiling for 5 min in the presence of 1% SDS followed by cooling on ice. To the denatured pLCAT or rLCAT (~120 pmol in 8 μl) were added 2 μL N-glycosidase F solution (0.2 U/μl, Boehringer Mannheim), 4 μl O-glycosidase solution (0.5 mU/μL, Boehringer Mannheim), 14 μL 5% nonidet P-40 (Sigma), and 36 μL 10 mM sodium phosphate buffer, pH 7.4. The mixture was incubated at 37°C for 17 h, and the products were analyzed by SDS-PAGE and mass spectroscopy.

Low resolution mass spectra of rLCAT and pLCAT before and after deglycosylation were obtained on a MALDI-TOF Mass Spectrometer (Micromass, Manchester, U.K.) using the matrix-assisted laser desorption ionization technique in the Mass Spectrometry Laboratory, School of Chemical Sciences, University of Illinois at Urbana-Champaign.

### Circular dichroism

CD spectra of rLCAT and pLCAT were recorded on a Jasco J-720 spectropolarimeter (Laboratory for Fluorescence Dynamics, University of Illinois at Urbana-Champaign) at 25°C with a water-jacketed CD cuvette of 1 mm path length (Helmer) in 5 mM sodium phosphate buffer (pH 7.4), 0.1 mM EDTA. Data were recorded for samples as well as blanks from 260 to 184 nm with 1 nm band width, 0.2 nm step size, 16 s response time, and a speed of 1 nm/min.

Secondary structural content was estimated using the self-consistent method (SELCON) by Sreerama and Woody (32, 33).

### Fluorescence spectroscopy

The intrinsic fluorescence emission spectra of pLCAT and rLCAT were obtained on a ISS PC1 Photon Counting Spectrofluorometer (Laboratory for Fluorescence Dynamics, University of Illinois at Urbana-Champaign) at 25°C from 310 to 450 nm with excitation at 295 nm, an integration time of 2 s, a step size of 1 nm, and excitation and emission band widths of 4 and 8 nm, respectively.

For the denaturation analysis, values of wavelength maxima of the intrinsic tryptophan fluorescence emis-

sion spectra were plotted versus the concentration of guanidine hydrochloride (GdnHCl). The primary data were then converted to a plot of $F_{app}$ (apparent fraction of unfolded protein) versus GdnHCl concentration and were fitted to an equation (34) relating $F_{app}$ with $\Delta G_{(H_2O)}$ (the free energy change of denaturation in the absence of GdnHCl) and m (the cooperativity of the transition).

## RESULTS

### rLCAT purification and enzymatic activity

Purification of rLCAT from the cell medium by phenyl Sepharose column chromatography gave a single protein peak. As assessed by SDS polyacrylamide gel electrophoresis, the protein peak contained only one major band (**Fig. 1A,** lane 2) with a molecular weight comparable to pLCAT. The yield of pure rLCAT from the cell medium was ~90% and the recovery ranged from 1.5 to 5.2 mg per liter of cell culture for three separate preparations, using two distinct cell lines. The kinetic parameters for the reaction of purified rLCAT and pLCAT are listed in **Table 1.** The catalytic rate constant (apparent $V_{max}$/enzyme concentration) is 2-fold larger for the pLCAT than for rLCAT, while the apparent $K_m$ is identical for both enzyme forms.

### Protein purity and N-terminal sequences

The purity of rLCAT was determined by SDS-PAGE as shown in Fig. 1. Purified rLCAT (Fig. 1A, lane 2) had one major broad band (>96% of the total stain intensity) that was identified as LCAT by Western blot analysis. The molecular weight of rLCAT, estimated by reference to the molecular weight standards, is approximately 73 kDa. The protein bands above the major LCAT band correspond to multimeric LCAT forms as indicated by Western blot analysis (Fig. 1C). The sharp band immediately below the broad rLCAT band represents the only contaminating protein accounting for <4% of total intensity. This protein band is separated from the rLCAT band only on the 7.5%, but not on the 12.5% SDS gel. Subsequent Western blot analysis showed that this contaminant is BSA, which can be easily removed by passing the preparation through an Affigel-blue column.

N-terminal sequencing of the major rLCAT band showed that purified rLCAT contains two sequences: one (60%) starts from Phe[1] and the other (40%) from Val[6]. The difference in molecular weight between these two sequences is ~0.6 kDa. It is not clear whether the presence of the shorter sequence is a result of intracellular processing or extracellular proteolytic cleavage. The same percentage of the truncated sequence was present when protease inhibitors, including leupeptin, pepstatin A, and EDTA, were added to the Opti-MEM medium or were added in the following purification steps. Serine protease inhibitors could not be used because LCAT has an active site serine itself. In any case, this polymorphism should not significantly affect the results obtained in this study, except for the reported number of isoforms for rLCAT.

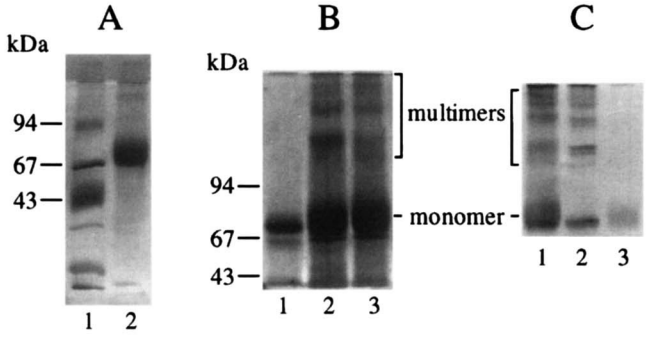


**Fig. 1.** Assessment of the purity of recombinant LCAT. Panel A: 12.5% SDS-PAGE PhastGel shows standard proteins (lane 1) and purified rLCAT (0.5 μg) (lane 2). Panel B: 7.5% SDS-PAGE PhastGel shows pLCAT (0.24 μg) (lane 1); rLCAT (1.8 μg) boiled before electrophoresis (lane 2); and rLCAT (1.8 μg) electrophoresed without boiling (lane 3). Panel C: 7.5% SDS-PAGE PhastGel detected by immunoblot. rLCAT (lane 1); pLCAT (lane 2); and 10-fold concentrated cell culture medium (lane 3). This panel demonstrates that the higher molecular weight bands present in the purified LCAT preparations in the preceding panels are multimeric forms of LCAT.

### Molecular weights and pI isoforms

The molecular weight of the plasma LCAT has been determined by various techniques in a number of laboratories. Values ranging from 65 to 68 kDa have been reported in the literature based on SDS-PAGE analysis (10, 14–16). Smaller values ranging from 59 to 63 kDa have been reported from sedimentation equilibrium ultracentrifugation analysis (11, 14, 15). In this study, the apparent molecular weight of monomeric LCAT was estimated on SDS-PAGE and is about 73 kDa for rLCAT and 71 kDa for pLCAT (**Table 2**); however, the rLCAT band on the SDS gel is significantly broader than that of pLCAT.

Molecular weight values obtained from SDS-PAGE are overestimated due to abnormal migration of highly glycosylated LCAT; therefore, mass spectra were obtained for both rLCAT and pLCAT to accurately determine their molecular weights. The peak width at half peak height is taken as the upper limit of the molecular weight range, giving a range from 57.3 to 64.6 kDa for rLCAT and from 55.7 to 59.6 kDa for pLCAT, and corresponding average molecular weights of ~61 and ~58 kDa, respectively (Table 2). In addition to a broader

TABLE 1. Purification of recombinant LCAT (rLCAT) and comparison of its kinetic parameters with plasma LCAT (pLCAT)

| | [Protein] ($\mu g\ ml^{-1}$) | $k_{cat}$[a] (nmol CE $h^{-1}\ \mu g^{-1}$) | Apparent $K_m$ (M) ($\times 10^7$) | $k_{cat}/K_m$ (nmol CE $h^{-1}\ \mu g^{-1}\ M^{-1}$) ($\times 10^{-8}$) |
|---|---|---|---|---|
| Medium[b] | 4.7 | | | |
| rLCAT[c] | 420 | 11.8 ± 0.1 | 1.11 ± 0.01 | 1.07 ± 0.2 |
| pLCAT[d] | 50 | 27.8 ± 0.4 | 1.14 ± 0.10 | 2.5 ± 0.2 |

[a]$k_{cat}$ = apparent $V_{max}$/enzyme concentration; the kinetic parameters are the average (± SD) from two experiments each performed in triplicate using rHDL substrates.

[b]Growth medium (Opti-MEM I) from permanently transfected CHO/*dhfr*$^-$ cells grown for 3 days on porous microcarrier beads. Total volume: 1 liter; total protein: 4.7 mg.

[c]Purified by phenyl Sepharose column chromatography. Total volume: 10 ml; total protein: 4.2 mg. The yield of purified LCAT is 90%.

[d]Purified from 2 liters of human plasma by a modification of previously described procedures (16, 31).

molecular weight range, rLCAT has a 3 kDa higher average value than pLCAT. The differences in the range and the average value between rLCAT and pLCAT cannot be accounted for by the presence of 40% of the shorter rLCAT sequence; therefore, these differences suggest that glycosylation in this recombinant LCAT is more extensive and more heterogeneous than in pLCAT. From the average molecular weights, rLCAT and pLCAT are calculated to have 23% and 19% of their respective total masses as carbohydrates.

Recombinant LCAT was denatured and deglycosylated, and its molecular weight was determined by mass spectrometry. This method gave a molecular weight of around 49 kDa, close to what is predicted from the primary sequence of LCAT (47.09 kDa) (4).

Information on the different charged forms of the fully glycosylated LCAT was obtained from measurements of the isoelectric points of rLCAT and pLCAT by isoelectric focusing. The rLCAT has at least 12 isoforms with pI values ranging from 4.0 to 5.4, while pLCAT has at least 9 isoforms with pI values ranging from 4.0 to 4.8. Thus, rLCAT has 3 extra isoforms in the range from 4.8 to 5.4.

TABLE 2. Physicochemical properties of recombinant LCAT (rLCAT) and plasma LCAT (pLCAT)

| | rLCAT | pLCAT |
|---|---|---|
| Average molecular weight[a] (kDa) | 61 | 58 |
| Molecular weight range[a] (kDa) | 57.3–64.6 | 55.7–59.6 |
| Number of pI Isoforms[b] | 12 | 9 |
| Range of pI values[b] | 4.0–5.4 | 4.0–4.8 |
| Extinction coefficient (280 nm)[c] | | |
| ($mg^{-1}\ cm^2$) | 2.0 | 2.0 |
| ($M^{-1}\ cm^{-1}$) | $9.4 \times 10^4$ | $9.4 \times 10^4$ |
| Fluorescence $\lambda_{max}$[d] (nm) | 335 | 335 |
| Secondary structure content[e] | | |
| (% α-helix; % β sheet; | | |
| % β turn; other) | 24; 42; 19; 15 | 25; 47; 18; 10 |
| Free energy of denaturation | | |
| ($\Delta G_{(H_2O)}$)[f] (kcal/mol) | 3.4 ± 0.2 | 3.2 ± −0.2 |
| Cooperativity of denaturation (m)[f] | | |
| (mg/ml · M [GdnHCl]) | −1.3 ± 0.2 | −1.2 ± 0.1 |

[a]From mass spectrometric analysis.

[b]From isoelectric focusing.

[c]Determined by the Edelhoch method (35, 36). The value with units of $mg^{-1}\ cm^2$ is calculated based on the polypeptide chain molecular mass (47.09 kDa).

[d]Wavelength of maximum fluorescence; from uncorrected emission spectra excited at 295 nm.

[e]From CD spectra analyzed using SELCON by Sreerama and Woody (32, 33).

[f]From the data in Fig. 4 fitted to the expression for $F_{app}$ vs. $\Delta G_{(H_2O)}$ and m (34).

## Self-association

As mentioned above, purified rLCAT samples boiled in 3% SDS show the presence of multimeric forms on SDS gels after cooling at room temperature or on ice (Fig. 1). Plasma LCAT also forms aggregates resistant to SDS.

To determine whether self-association also occurs in the native state, the association states of rLCAT and pLCAT were probed under native conditions by native gradient polyacrylamide gel electrophoresis (**Fig. 2A**). At a 9.6 μM (0.45 mg/ml) protein concentration, a total of six bands were observed for rLCAT, the monomeric rLCAT accounting for 53% of the total intensity. The higher molecular weight bands are presumably multimeric forms of rLCAT; their relative intensities range from 12% to 6% of the total stain intensity. Under the same native conditions and at a concentration 7-fold lower than that of rLCAT, pLCAT also contains multimers (32%) in addition to the monomer form (68%). The fact that the multimeric forms were detected on native gels without covalent cross-linking indicates that the intermolecular interactions responsible for the formation of multimeric forms in the native state are strong for both rLCAT and pLCAT.

The formation of multimeric LCAT forms and their relative amounts were also analyzed by chemical cross-linking using two cross-linkers with different spacer arm lengths followed by SDS gel electrophoresis on 8–25%

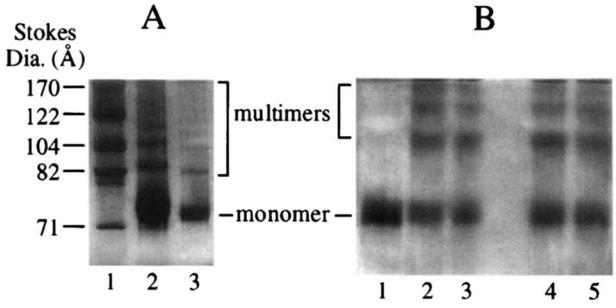


**Fig. 2.** Multimeric forms of LCAT. Panel A: non-denaturing 8–25% polyacrylamide gradient electrophoresis of standard proteins with their corresponding Stokes diameters (lane 1); rLCAT (0.45 μg) (lane 2); and pLCAT (0.06 μg) (lane 3). One-μl samples of both LCAT forms were analyzed. Panel B: 7.5% SDS PhastGel of chemically cross-linked LCAT. Concentrated rLCAT (1.0 mg/ml) was diluted to 0.75, 0.60, 0.20, and 0.01 mg/ml (lanes 2, 3, 4, and 5, respectively) and was cross-linked with Sulfo-EGS. Unreacted rLCAT (lane 1). After reaction, the same amount of protein was applied to each lane for electrophoretic analysis.

gradient gels (Fig. 2B). Using $BS^3$ as the cross-linker (spacer arm length: 11.4 Å), 60 ± 5% of rLCAT formed various multimers. When using sulfo-EGS as the cross-linker which has a longer spacer arm (16.1 Å), the amount of rLCAT in multimeric forms was 56 ± 5%. Thus, the two cross-linkers gave similar percentage of rLCAT in multimeric forms, an average of 58 ± 5%, which is close to 47 ± 4% found on native gels without cross-linking. Thus, it can be reasonably concluded that at a concentration of 0.45 mg/ml, 53 ± 5% of rLCAT exists as a monomer and the rest forms various multimers.

The concentration dependence of the monomer and multimer composition was studied for rLCAT by cross-linking experiments using sulfo-EGS in the concentration range from 0.010 to 0.75 mg/ml. The electrophoresis results for these samples are shown in Fig. 2B. No concentration dependence was observed in the 75-fold concentration range studied, although the presence of both monomer and multimers suggests that the system is within a concentration range where an equilibrium shift may be expected with a shift in total protein concentration. This result suggests that the aggregation is very slowly reversible or essentially irreversible.

### Spectroscopic properties of rLCAT and pLCAT

The extinction coefficients were determined for both recombinant and plasma LCAT by the methods of Edelhoch (35) and Gill and von Hippel (36) which generally give more reliable result than other methods (37). As listed in Table 2, the extinction coefficient of both rLCAT and pLCAT is $9.4 \times 10^4\ M^{-1}\,cm^{-1}$ in 5 mM sodium phosphate buffer (pH 7.4) and 5 mM EDTA, or $2.0\ mg^{-1}\,cm^2$, which matches the literature values of $2.0–2.1\ mg^{-1}\,cm^2$ determined using various methods including amino acid composition analysis, the Lowry method and the Edelhoch method (5, 12, 14). It should be noted that the value in $mg^{-1}\,cm^2$ was obtained when 47,090, the polypeptide molecular weight (not including the carbohydrate), was used.

The intrinsic fluorescence spectra (**Fig. 3A**) for rLCAT and pLCAT, measured at 0.05 mg/ml, were essentially identical in terms of intensity, shape, and $\lambda_{max}$ (335 nm). Similarly, the CD spectra for rLCAT and pLCAT, measured at 0.05 mg/ml, were very comparable in their shapes and intensities (Fig. 3B). Even though the minimum between 210 and 218 nm is about 10% less intense for rLCAT, the estimated contents of secondary structure are similar: 24–25% α-helix, 42–47% β-sheet, 18–19% turn, and 10–15% other structure (see Table 2).

Protein stability was determined by GdnHCl denaturation monitored by intrinsic tryptophan fluorescence of LCAT at 0.049 mg/ml. The LCAT monomer contains

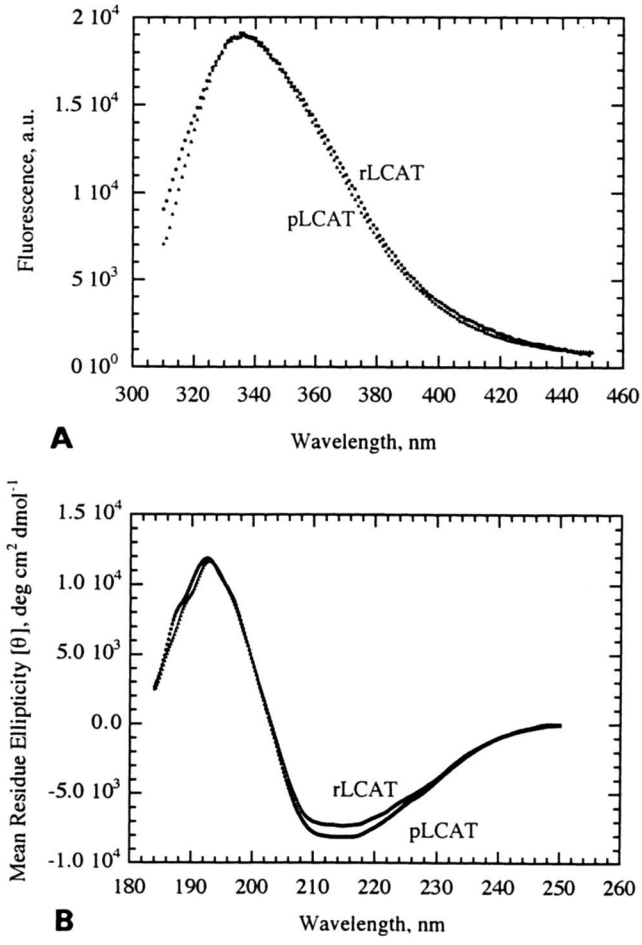


**Fig. 3.** Flourescence and circular dichroism spectra of rLCAT and pLCAT (0.05 mg/ml). Panel A: uncorrected fluorescence spectra excited at 295 nm. Panel B: circular dichroism spectra.

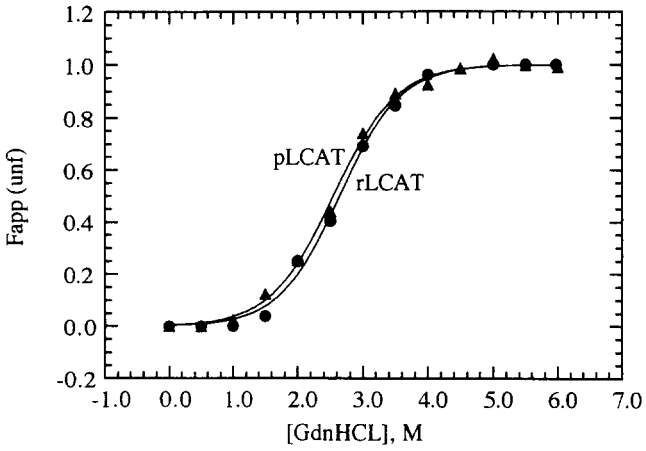


**Fig. 4.** Denaturation of recombinant LCAT and plasma LCAT with GdnHCl. Wavelengths of maximum fluorescence (excited at 295 nm) were obtained at equilibrium for each GdnHCl concentration, and the apparent fraction of unfolded protein ($F_{app}$) was calculated. The curves are theoretical fits to an equation relating $F_{app}$ to $\Delta G_{(H_2O)}$ and m (the measure of cooperativity) (34).

12 tryptophans; and, thus, the observed fluorescence $\lambda_{max}$ represents an average environment of all 12 Trp residues. Data in the form of apparent fraction of unfolded protein ($F_{app}$) versus GdnHCl concentration were fitted to an equation derived by assuming a two-state transition from native monomer to unfolded monomer (34), from which $\Delta G_{(H_2O)}$ and m values were obtained (**Fig. 4**). The $\Delta G_{(H_2O)}$ of rLCAT is 3.4 ± 0.2 kcal/mol at 25°C, and the m value is −1.3 mg/ml · M (GdnHCl); for pLCAT, $\Delta G_{(H_2O)}$ is 3.2 ± 0.2 kcal/mol, and the m value is −1.2 mg/ml · M (GdnHCl) (Table 2).

## DISCUSSION

In this study, we overexpressed recombinant human LCAT in CHO/*dhfr*$^-$ cells, and purified to homogeneity (>96% purity) up to 5 mg of enzyme which has 42% of the specific activity of pLCAT. Clearly, this animal cell expression system is suitable for the production of enzymatically active LCAT (and LCAT mutants) in sufficient amounts for structural and stability studies. Hill et al. (28) previously reported the permanent expression and secretion of human LCAT by BHK cells and its purification using a one-step phenyl Sepharose column procedure that we adapted in this work. However, in addition, our study includes an extensive physicochemical characterization of the rLCAT and a detailed comparison with pLCAT in terms of molecular weight, degree of glycosylation, kinetic parameters (apparent $V_{max}$ and apparent $K_m$), number of pI isoforms, N-terminal sequence analysis, degree of self-association, CD and fluorescence spectral properties, and protein stability.

Overall, the recombinant LCAT has properties very similar to plasma LCAT. However, compared to pLCAT, rLCAT has a higher average molecular weight (by 3 kDa) and also a broader range of molecular weights as determined by mass spectrometry. A broader molecular weight range compared to pLCAT was also observed for rLCAT from BHK cells by Hill et al. (28). Complete deglycosylation of our rLCAT resulted in a single sharp band on mass spectrometry whose molecular weight matched that of the pLCAT polypeptide chain, indicating that the molecular weight differences between rLCAT and pLCAT must be due to differences in their carbohydrate contents. It has been recently shown that LCATs from different sources (human plasma or different cell lines) have distinct enzymatic activities, and these differences have been attributed to the differences in their carbohydrate structures (38). In this study, the rLCAT from CHO cells was also shown to have a lower specific activity (42%) than pLCAT. This difference in enzymatic activity is due to differences in apparent $V_{max}$ rather than in apparent $K_m$ values. The identical apparent $K_m$ values suggest that the interfacial binding constants are also identical (39) for both forms of the enzyme. Therefore, the differences in glycosylation probably do not affect the interaction of LCAT with lipoprotein surfaces. The decreased catalytic rate of the rLCAT could be due to a decreased catalytic efficiency, related to the glycosylation pattern. To test this hypothesis, we attempted to produce deglycosylated LCAT for measurements of enzyme kinetics; however, extensive deglycosylation gave insoluble protein.

To assess how well the mass spectroscopic results represent the average molecular weight and weight distribution of LCAT, we calculated the expected molecular weight and range for pLCAT from the known polypeptide molecular weight (47.09 kDa) and the carbohydrate chain compositions reported by Schindler et al. (13). The major species of glycosylated LCAT, as calculated from Schindler et al. (13) would have a molecular weight of 60.3 kDa, and the range would be from 58.2 to 63.5 kDa. By comparison, our experimentally determined average molecular weight is 58 kDa, and the range is from 55.7 to 59.6 kDa. Although the absolute measured and calculated values are shifted by 2 to 3 kDa, the widths of the distributions are comparable and lend support for our conclusion that the width of the mass spectrum represents the distribution of glycosylated pLCAT and rLCAT forms. We also calculate that the average content of carbohydrate in pLCAT is closer to 19–22% than to the 25% figure widely reported in the literature.

In addition to the isoforms of LCAT arising due to

differences in sialic acid content, we found that rLCAT has two distinct polypeptide forms, one with an N-terminus at the expected Phe for mature LCAT, and another at Val[6]. The origin and functional significance of the latter variant are not yet known, but may be due to intracellular processing or extracellular proteolysis of rLCAT in the CHO cell system. Evidently, this modification increases the observed isoforms for rLCAT, but does not seem to affect the protein structure nor stability. Very likely it does not affect the enzymatic activity of rLCAT, as well. This assertion is based on our observation (unpublished results, Adimoolam and A. Jonas, 1995) that pLCAT which has been digested with trypsin and has lost 16 of its amino terminal residues, retains almost full enzymatic activity.

In this study, we have demonstrated, for the first time, that LCAT self-associates at concentrations greater than 0.4 mg/ml. The multimers persist upon dilution and are resistant to dissociation by SDS, suggesting that the association is irreversible or that the multimers have very slow dissociation kinetics. A practical conclusion is that attempts to crystallize LCAT would be hampered, not only by the heterogeneity of the glycosylated protein, but also by its tendency to aggregate at the high concentrations usually required for crystallization. Furthermore, attempts to crystallize deglycosylated LCAT would have a very small chance of success because the solubility of LCAT would be decreased, and the tendency to aggregate increased further in the enzyme devoid of carbohydrate. The functional impact of LCAT self-association/aggregation is not evident. At the low concentrations of LCAT in plasma (~6 mg/L) (40), the enzyme is probably present as a monomer, but as it binds to lipoprotein surfaces, its local concentration would increase greatly and may result in self-association. Regarding enzymatic activity, aggregated forms of LCAT would probably have impaired enzymatic activity because lipid binding hydrophobic regions involved in protein–protein contacts would not be available for, or would interfere with, binding to interfacial substrates. Thus, the difference in the specific activities between pLCAT and rLCAT could be due, in part, to the presence of different amounts of aggregated LCAT.

The spectral properties and stabilities of rLCAT and pLCAT compared by CD and fluorescence methods are very similar, consistent with similar, if not identical protein structures. The fluorescence $\lambda_{max}$ of 335 nm indicates that the 12 Trp residues of LCAT are, on average, located in a relatively nonpolar environment. The content of secondary structure, for both forms of the enzyme, is similar to that reported previously by other laboratories based on CD measurements (14, 15) or predicted from the primary sequence (4, 6). The stability of LCAT ($\Delta G_{(H_2O)}$) is reported for the first time in this study. The value of 3.2–3.4 kcal/mol obtained from the denaturation experiments with GdnHCl (midpoint of denaturation at 2.6 M GdnHCl) is low compared to the more typical value of ~10 kcal/mol for globular, water-soluble proteins. The low $\Delta G_{(H_2O)}$ for LCAT is closer to the 2.4 kcal/mol value reported for apoA-I (41), probably reflecting the potential for conformational changes upon binding to lipoproteins.

This study of the physicochemical properties of pure recombinant LCAT sets the stage for ongoing structure–function investigations of mutant LCAT forms with altered interfacial binding, or activation properties.

This work was supported by NIH grant HL 29939 to A. Jonas. We gratefully acknowledge the gift of LCAT cDNA by Genentech Co., the gift of anti-LCAT antibodies by Dr. H. Pownall (Baylor College of Medicine), and the assistance of Shanthi Adimoolam (University of Illinois) in the production and maintenance of the permanently transfected CHO/*dhfr*$^-$ cell lines.

*Manuscript received 8 October 1996 and in revised form 24 February 1997.*

## REFERENCES

1. Jonas, A. 1987. Lecithin:cholesterol acyltransferase. *In* Plasma Proteins. A. M. Gotto, Jr., editor. Elsevier Science Publishers B. V. (Bomedical Division). 299–333.
2. Jonas, A. 1991. Lecithin-cholesterol acyltransferase in the metabolism of high-density lipoproteins. *Biochim. Biophys. Acta.* **1084:** 205–220.
3. Fielding, C. J., and P. E. Fielding. 1995. Molecular physiology of reverse cholesterol transport. *J. Lipid Res.* **36:** 211–228.
4. McLean, J., C. Field, D. Drayna, H. Dieplinger, B. Baer, W. Kohr, W. Henzel, and R. Lawn. 1986. Cloning and expression of human lecithin-cholesterol acyltransferase cDNA. *Proc. Natl. Acad. Sci. USA.* **83:** 2335–2339.
5. Yang, C-Y., D. Manoogian, Q. Pao, F-S. Lee, R. D. Knapp, A. M. Gotto, and H. J. Pownall. 1987. Lecithin:cholesterol acyltransferase: functional regions and a structural model of the enzyme. *J. Biol. Chem.* **262:** 3086–3091.
6. Fielding, C. J. 1990. Lecithin:cholesterol acyltransferase. *In* Advances in Cholesterol Research. M. Esfahani and J. Swaney, editors. Telford Press, Caldwell, NJ. 270–314.
7. Francone, O. L., L. Evangelista, and C. J. Fielding. 1992. Lecithin-cholesterol acyltransferase: effects of mutagenesis at N-linked oligosaccharide attachment sites on acyl acceptor specificity. *Biochim. Biophys. Acta.* **1166:** 301–304.
8. O, K., J. S. Hill, X. Wang, R. Mcleod, and P. H. Pritchard. 1993. Lecithin:cholesterol acyltransferase: role of N-linked glycosylation in enzyme function. *Biochem. J.* **294:** 879–884.
9. Qu, S-J., H-Z. Fan, F. Blanco-Vaca, and H. J. Pownall. 1993. Effects of site-directed mutagenesis on the N-glycosylation sites of human lecithin:cholesterol acyltransferase. *Biochemistry.* **32:** 8732–8736.
10. Albers, J. J., J. T. Lin, and G. P. Roberts. 1979. Effect of human plasma apolipoprotein on the activity of purified lecithin:cholesterol acyltransferase. *Artery.* **5:** 61–75.
11. Chung, J., D. A. Abano, G. M. Fless, and A. M. Scanu. 1979. Isolation, properties, and mechanism of in vitro ac-

tion of lecithin:cholesterol acyltransferase from human plasma. *J. Biol. Chem.* **254:** 7456–7464.
12. Chong, K. S., M. Jahani, S. Hara, and A. G. Lacko. 1983. Characterization of lecithin-cholesterol acyltransferase from human plasma. 3. Chemical properties of the enzyme. *Can. J. Biochem.* **61:** 875–881.
13. Schindler, P. A., C. A. Settineri, X. Collet, C. J. Fielding, and A. L. Burlingame. 1995. Site-directed detection and structural characterization of the glycosylation of human plasma proteins lecithin:cholesterol acyltransferase and apolipoprotein D using HPLC/electrospray mass spectrometry and sequential glycosidase digestion. *Protein Sci.* **4:** 791–803.
14. Doi, Y., and T. Nishida. 1983. Microheterogeneity and physical properties of human lecithin-cholesterol acyltransferase. *J. Biol. Chem.* **258:** 5840–5846.
15. Chong, K-S., S. Hara, R. E. Thompson, and A. G. Lacko. 1983. Characterization of lecithin:cholesterol acyltransferase from human plasma. II. Physical properties of the enzyme. *Arch. Biochem. Biophys.* **222:** 553–560.
16. Albers, J. J., V. G. Cabana, and Y. D. Barden Stahl. 1976. Purification and characterization of human plasma lecithin:cholesterol acyltransferase. *Biochemistry.* **15:** 1084–1087.
17. Furukawa, Y., and T. Nishida. 1979. Stability and properties of lecithin-cholesterol acyltransferase. *J. Biol. Chem.* **254:** 7213–7219.
18. Francone, O. L., and C. J. Fielding. 1991. Structure–function relationships in human lecithin:cholesterol acyltransferase. Site-directed mutagenesis at serine residues 181 and 216. *Biochemistry.* **30:** 10074–10077.
19. Francone, O. L., and C. J. Fielding. 1991. Effects of site-directed mutagenesis at residues cysteine-31 and cysteine-184 on lecithin-cholesterol acyltransferase activity. *Proc. Natl. Acad. Sci. USA.* **88:** 1716–1720.
20. Funke, H., A. von Eckardstein, P. H. Pritchard, J. J. Albers, J. J. P. Lastelein, C. Droste, and G. Assmann. 1991. A molecular defect causing fish eye disease: an amino acid exchange in lecithin-cholesterol acyltransferase (LCAT) leads to the selective loss of α-LCAT activity. *Proc. Natl. Acad. Sci. USA.* **88:** 4855–4859.
21. Gotoda, T., N. Yamada, T. Murse, M. Sakuma, N. Murayama, H. Shimano, K. Kozaki, J. J. Albers, Y. Yazaki, and Y. Akanuma. 1991. Differential phenotypic expression by three mutant alleles in familial lecithin:cholesterol acyltransferase deficiency. *Lancet.* **338:** 778–781.
22. Funke, H., A. von Eckardstein, P. H. Pritchard, A. E. Hornby, H. Wiebusch, C. Motti, M. R. Hayden, C. Dachet, B. Jacotot, U. Gerdes, O. Faergeman, J. J. Albers, N. Colleoni, A. Catapano, J. Frohlich, G. Assmann, M. Kleingunnewigk, and A. Reckerth. 1993. Genetic and phenotypic heterogeneity in familial lecithin-cholesterol acyltransferase (LCAT) deficiency: 6 newly identified defective alleles further contribute to the structural heterogeneity in this disease. *J. Clin. Invest.* **91:** 677–683.
23. Klein, H-G., P. Lohse, N. Duverger, J. J. Albers, D. J. Rader, L. A. Zech, S. Santamarina-Fojo, and H. B. Brewer, Jr. 1993. Two different allelic mutations in the lecithin:cholesterol acyltransferase (LCAT) gene resulting in classic LCAT deficiency: LCAT ($tyr^{83} \rightarrow$ stop) and LCAT ($tyr^{156} \rightarrow$ asn). *J. Lipid Res.* **34:** 49–58.
24. Klein, H-G., N. Duverger, J. J. Albers, S. Marcovina, H. B. Brewer, and S. Santamarina-Fojo. 1995. In vitro expression of structural defects in the lecithin-cholesterol acyltransferase gene. *J. Biol. Chem.* **270:** 9443–9447.
25. Qu, S. J., H-Z. Fan, F. Blanco-Vaca, and H. J. Pownall. 1995. In vitro expression of natural mutants of human lecithin:cholesterol acyltransferase. *J. Lipid Res.* **36:** 967–974.
26. Lee, Y-P., S. Adimoolam, M. Liu, P. V. Subbaiah, K. Glenn, and A. Jonas. 1997. Analysis of human lecithin cholesterol acyltransferase activity by carboxyl-terminal truncation. *Biochim. Biophys. Acta.* **1344:** 250–261.
27. Subbaiah, P. V., M. Liu, J. Senz, X. B. Wang, and P. H. Pritchard. 1994. Substrate and positional specificities of human and mouse lecithin-cholesterol acyltransferases. Studies with wild type recombinant and chimeric enzymes expressed in vitro. *Biochim. Biophys. Acta.* **1215:** 150–156.
28. Hill, J. S., K. O, X. Wang, S. Paranjape, D. Dimitrijevich, A. G. Lacko, and P. H. Pritchard. 1993. Expression and characterization of recombinant human lecithin:cholesterol acyltransferase. *J. Lipid Res.* **34:** 1245–1251.
29. Matz, C. E., and A. Jonas. 1982. Micellar complexes of human apolipoprotein A-I with phosphatidylcholine and cholesterol prepared from cholate-lipid dispersions. *J. Biol. Chem.* **257:** 4535–4540.
30. Jonas, A. 1986. Reconstitution of high-density lipoproteins. *Methods Enzymol.* **128:** 553–582.
31. Matz, C. E., and A. Jonas. 1982. Reaction of human lecithin:cholesterol acyltransferase with synthetic micellar complexes of apolipoprotein A-I, phosphatidylcholine, and cholesterol. *J. Biol. Chem.* **257:** 4541–4546.
32. Sreerama, N., and R. W. Woody. 1993. A self-consistent method for the analysis of protein secondary structure from circular dichroism. *Anal. Biochem.* **209:** 32–44.
33. Sreerama, N., and R. W. Woody. 1994. Poly(pro)II helices in globular proteins: identification and circular dichroic analysis. *Biochemistry.* **33:** 10022–10025.
34. Aune, K. C., and C. Tanford. 1969. Thermodynamics of the denaturation of lysozyme by guanidine hydrochloride. *Biochemistry.* **8:** 4586–4590.
35. Edelhoch, H. 1967. Spectroscopic determination of tryptophan and tyrosine in proteins. *Biochemistry.* **6:** 1948–1954.
36. Gill, S. C., and P. H. von Hippel. 1989. Calculation of protein extinction coefficients from amino acid sequence data. *Anal. Biochem.* **182:** 319–326.
37. Pace, C. N., F. Vajdos, L. Fee, G. Grimsley, and T. Gray. 1995. How to measure and predict the molar absorption coefficient of a protein. *Protein Sci.* **4:** 2411–2423.
38. Miller, K. R., J. Wang, M. Sorci-Thomas, R. A. Anderson, and J. S. Parks. 1996. Glycosylation structure and enzyme activity of lecithin:cholesterol acyltransferase from human plasma, HepG2 cells, and baculoviral and Chinese hamster ovary cell expression system. *J. Lipid Res.* **37:** 551–561.
39. Bolin, D. J., and A. Jonas. 1994. Binding of lecithin:cholesterol acyltransferase to reconstituted high density lipoproteins is affected by their lipid but not apolipoprotein composition. *J. Biol. Chem.* **269:** 7429–7434.
40. Albers, J. J., C. Chen, and J. L. Adolphson. 1981. Lecithin:cholesterol acyltransferase mass; its relationship to LCAT activity and cholesterol esterification rate. *J. Lipid Res.* **22:** 1206–1213.
41. Tall, A. R., D. M. Small, G. G. Shipley, and R. S. Lees. 1975. Apoprotein stability and lipid–protein interactions in human plasma high density lipoproteins. *Proc. Natl. Acad. Sci. USA.* **72:** 4940–4942.